^{24}Mg(^{16}O,^{12}C)^{28}Si and ^{24}Mg(^{16}O,^{16}O)^{24}Mg reactions at backward angles

M. Paul, S. J. Sanders, D. F. Geesaman, W. Henning, D. G. Kovar, C. Olmer,* and J. P. Schiffer

Argonne National Laboratory, Argonne, Illinois 60439

J. Barrette and M. J. LeVine

Brookhaven National Laboratory, Upton, New York 11973

(Received 29 October 1979)

Excitation functions of the ^{24}Mg(^{16}O,^{12}C)^{28}Si and ^{24}Mg(^{16}O,^{16}O)^{24}Mg reactions to the ground states and first-excited 2^+ states in ^{28}Si and ^{24}Mg have been measured at $\theta_{c.m.} = 180°$ over the energy range $24 \le E_{c.m.} \le 40$ MeV, where the ^{24}Mg(^{16}O,^{12}C)^{28}Si reaction is known to exhibit a strong resonant behavior at forward angles. The four measured excitation functions show prominent structures, about 1 MeV wide, strongly correlated in the elastic and inelastic channels. Angular distributions in the range $110° \le \theta_{c.m.} \le 180°$ were measured at $E_{c.m.} = 27.8$, 30.8, and 36.2 MeV. At 27.8 and 36.2 MeV, where prominent peaks exist in the (^{16}O,^{12}C) backward-angle excitation function, the angular distributions of the transfer to the 0^+ ground state are strongly rising toward 180° and have an oscillatory shape. The partial waves $L = (20,22)$ and 26, respectively, are predominant at these two energies. At 30.8 MeV the data indicate the interference between odd and even partial waves.

NUCLEAR REACTIONS ^{24}Mg(^{16}O,^{12}C), ^{24}Mg(^{16}O,^{16}O) $E_{c.m.} = 24-40$ MeV; measured $\sigma(E,\theta)$; correlation analysis; DWBA and P_L^2 analyses; deduced J values.

I. INTRODUCTION

The resonance-like behavior observed in heavy-ion systems involving s-d shell nuclei has raised much interest as to its origin and the possible new physical insight it may provide. The elastic and inelastic scattering cross sections for the systems ^{16}O+^{28}Si and ^{12}C+^{28}Si,[1] for example, show pronounced structures in their excitation functions at backward angles; at maxima of the excitation functions, the cross sections are strongly enhanced above the values expected from conventional optical-model calculations and have oscillatory angular distributions. The angular momenta of the dominant partial waves, as deduced from the shapes of the angular distributions, are close to the values obtained for the grazing partial waves in optical-model calculations. Lee et al.[2] have observed the same phenomena in a study of the ^{24}Mg(^{16}O,^{12}C)^{28}Si reaction at backward angles.

In the forward-angle region, resonant behavior has been observed in transfer reactions involving similar heavy-ion systems.[3-6] The excitation function of the reaction ^{24}Mg(^{16}O,^{12}C)^{28}Si at forward angles[3] in the range $23 \le E_{c.m.} \le 38$ MeV shows four evenly spaced structures. Direct transfer calculations, which can reproduce the shapes of the angular distributions at forward angles, do not account for the experimental energy dependence of the cross sections.

The physical origin of the observed phenomena is not yet understood. Several interpretations[1,7]

have been proposed for the backward-angle behavior of the elastic scattering in the systems mentioned above, primarily based on the occurrence of shape resonances in the heavy-ion potentials. No such model as yet is capable of explaining or reproducing the resonant behavior observed at forward angles. If resonance mechanisms are responsible for these phenomena, they should be dominant in the backward-angle region where the direct-transfer processes are expected to be weak. The motivation of the present work was to study the behavior of the ^{24}Mg(^{16}O, ^{12}C)^{28}Si reaction as well as that of the ^{24}Mg+^{16}O elastic and inelastic scattering at backward angles in the energy region where resonances were seen at forward angles. Such a study will explore the correlations between the forward- and backward-angle reaction excitation functions as well as the possible correlations among the reaction and elastic channel excitation functions. Taken together these data may provide an insight into the reaction mechanism.

Excitation functions of the ^{24}Mg(^{16}O, ^{12}C)^{28}Si reaction to the ground state and 1.78-MeV, 2^+ state in ^{28}Si and of the ^{24}Mg(^{16}O, ^{16}O)^{24}Mg elastic scattering and inelastic scattering to the 1.37-MeV, 2^+ state in ^{24}Mg were measured at $\theta_{c.m.} = 180°$ between $E_{c.m.} = 24$ and 40 MeV.[8] At $E_{c.m.} = 27.8$, 30.8, and 36.2 MeV, angular distributions for the same reactions were obtained over the angular range $130° \le \theta_{c.m.} \le 180°$ and used to establish limits on the angular momenta of the dominant partial waves. In the following paper,[10] the ground-state

transfer data are discussed within the framework
of resonant amplitudes added to a direct reaction
background.

II. EXPERIMENTAL METHOD AND RESULTS

In order to measure the excitation functions and
angular distributions for the ^{24}Mg(^{16}O, ^{12}C)^{28}Si and
^{24}Mg(^{16}O, ^{16}O)^{24}Mg reactions at backward angles,
the kinematically reversed reactions were studied
with ^{24}Mg as the projectile and the lighter outgoing
ions detected at forward angles. Beams of ^{24}Mg
in the energy range of 60–100 MeV were obtained
from the Brookhaven National Laboratory (BNL)
tandem Van de Graaff facility. Self-supporting
Al_2O_3 targets, about 70 μg/cm^2 thick, were used.
The outgoing ions were momentum analyzed at
forward angles in the BNL quadrupole-triple-di-
pole (QDDD) magnetic spectrometer. The focal-
plane detection system, described in Ref. 1, con-
sisted of a double-wire proportional counter. The
ions were stopped in the gas counter and generated
signals for position, differential energy loss, and
residual energy; unambiguous identification of
^{12}C or ^{16}O ions was possible.

For measurements at and near $\theta_{lab} = 0°$, the de-
tector was shielded from the primary ^{24}Mg beam
by metallic gold and Havar absorber foils. The
thickness of the absorber was varied over the
range 3–25 mg/cm^2 so that the ^{12}C or ^{16}O ions
retained sufficient energy to be identified in the
counter. For the detection of ^{16}O ions, an addi-
tional nickel foil of 1.7 mg/cm^2 thickness was
placed at the entrance aperture of the spectro-
graph. This foil removed the degeneracy in mag-
netic rigidity between elastically scattered ^{16}O
ions and one of the charge states of the primary
^{24}Mg beam and reduced the background contribu-
tion. In all these measurements, the ^{12}C or ^{16}O
groups corresponding to the ground- and first-
excited states in ^{28}Si or ^{24}Mg were well resolved.
Figure 1 shows the ^{12}C and ^{16}O energy spectra
taken at $\theta_{lab} = 0°$ with an incident ^{24}Mg beam energy
of 90.0 MeV.

For relative normalization purposes, a thin
layer of gold (~5 μg/cm^2) was evaporated onto
the AL_2O_3 targets. ^{24}Mg nuclei elastically scat-
tered from gold were counted in two out-of-plane
monitor detectors symmetrically located at 18°
with respect to the beam. The ratio of the yields
in the two detectors was used to monitor the in-
cident beam direction. Absolute cross sections
were obtained by normalizing the spectrometer
yields to the Rutherford elastic scattering of ^{24}Mg
by the oxygen target at $E_{lab} = 60.0$ MeV over labor-
atory angles from 13° to 19°. Charge state correc-
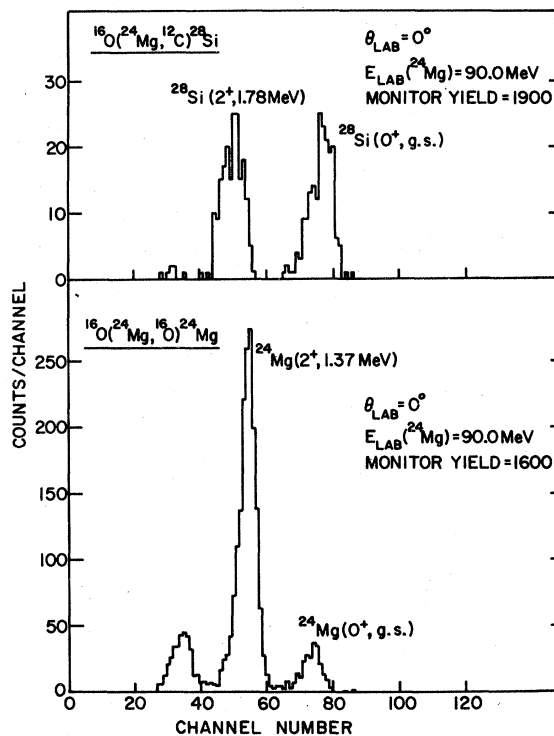tions to the ^{16}O yields, extrapolated from mea-

FIG. 1. Position spectra of the ^{12}C and ^{16}O groups
from the ^{16}O(^{24}Mg,^{12}C)^{28}Si and ^{16}O(^{24}Mg,^{16}O)^{24}Mg reac-
tions, respectively, measured in the focal plane of the
BNL-QDDD spectrometer at 0° and an incident labora-
tory energy of 90.0 MeV.

surements at incident laboratory energies of 70
and 86 MeV, were applied to the data. The es-
timated errors in the relative normalizations are
included in the figures; the error on the absolute
scale is about 25%.

Excitation functions for the ^{12}C and ^{16}O groups
corresponding to the ground- and first-excited
states in ^{28}Si and ^{24}Mg were measured at $\theta_{lab} = 0°$
with beam energies from 60 to 100 MeV in steps
of 0.750 MeV. The square-shaped spectrometer
aperture subtended in-plane angles of ±3°, cor-
responding to center-of-mass angles for the
^{24}Mg(^{16}O, ^{12}C)^{28}Si and ^{24}Mg(^{16}O, ^{16}O)^{24}Mg reactions of
180°±5° and 180°±6°, respectively. The experi-
mental excitation functions are plotted in Fig. 2.
They show a series of strong maxima about 1 MeV
wide with peak-to-valley ratios as large as 10.

At $E_{c.m.} = 27.8$, 30.8, and 36.2 MeV, angular dis-
tributions of the ^{12}C groups leading to the ground
state and first-excited 2$^+$ state in ^{28}Si were mea-
sured over the range 145° ≤ $\theta_{c.m.}$ ≤ 180°. At 30.8
MeV, the yield of the reaction is low and the above
aperture (±3°) was used; at other energies, angul-
ar distributions were measured with a rectangular
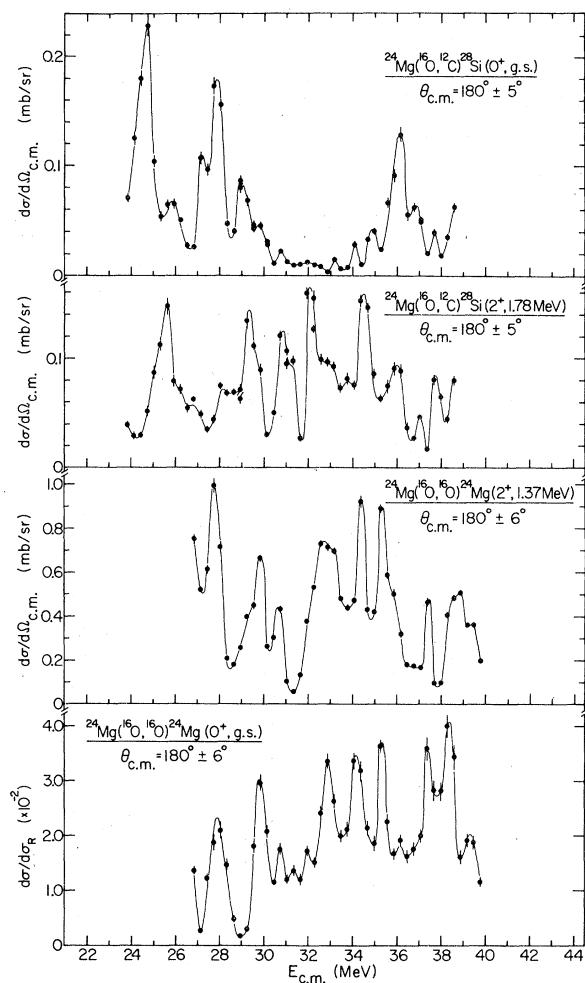aperture subtending ±0.5°. The reaction angle was

FIG. 2. Excitation functions for the indicated reactions at $\theta_{c.m.} = 180°$. The solid lines connect smoothly the experimental points.

FIG. 3. Backward angular distributions of the $^{24}Mg(^{16}O,^{12}C)^{28}Si(0^+,g.s.)$ and $^{24}Mg(^{16}O,^{12}C)^{28}Si(2^+,1.78$ MeV) reactions at the indicated energies. Vertical bars show the relative errors. Horizontal bars, where shown, represent the experimental angular aperture. The solid lines represent squared Legendre polynomials with the L values shown, normalized to fit the data.

determined with an accuracy of $\pm 0.07°$ by performing left and right measurements of the spectrometer yields. The experimental results for the $(^{16}O,^{12}C)$ reaction are shown in Fig. 3; in this figure, the vertical bars indicate the relative errors in the cross sections and, for the large-aperture measurements, the horizontal bars indicate the center-of-mass aperture angles.

Elastic and inelastic scattering angular distributions were measured in the backward hemisphere at $E_{c.m.} = 27.8$ MeV and $E_{c.m.} = 36.2$ MeV. At $E_{c.m.} = 27.8$ MeV, additional measurements were performed to establish the angular distribution over the full angular range. In these measurements, a self-supporting ^{24}Mg target of 120 $\mu g/cm^2$ thickness was bombarded by an ^{16}O beam from the Argonne National Laboratory FN tandem Van de Graaff. Depending on the scattering angle, ^{24}Mg
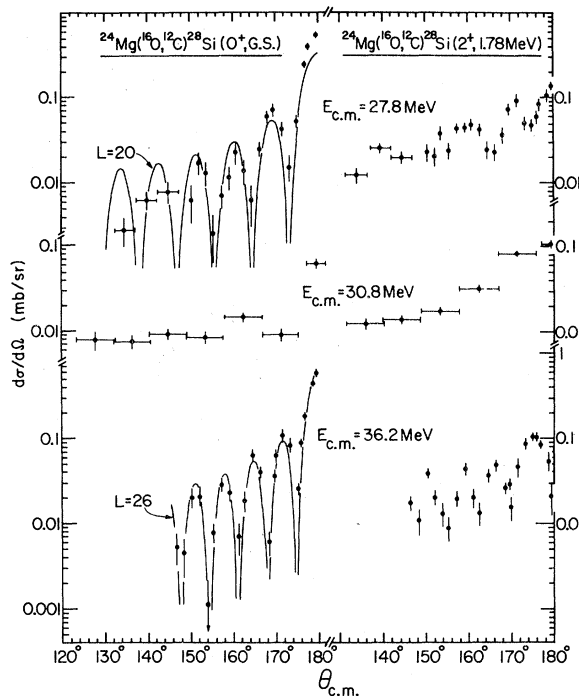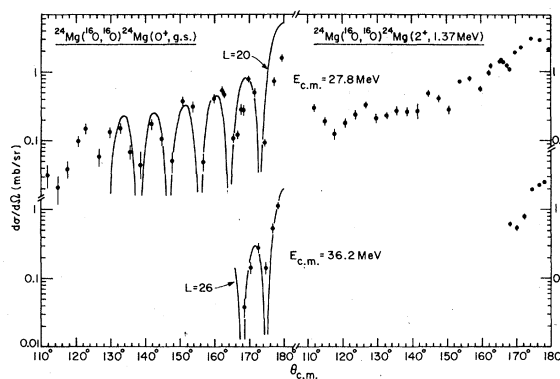

FIG. 4. Backward angular distributions of the $^{24}Mg(^{16}O,^{16}O)^{24}Mg(0^+,g.s.)$ and $^{24}Mg(^{16}O,^{16}O)^{24}Mg(2^+,1.37$ MeV) reactions at the indicated energies. The cross sections were obtained from the $^{16}O(^{24}Mg,^{16}O)^{24}Mg$ reaction for $160° \leqslant \theta_{c.m.} \leqslant 180°$ and the $^{24}Mg(^{16}O,^{24}Mg)^{16}O$ reaction for $110° \leqslant \theta_{c.m.} \leqslant 170°$. Vertical bars show the relative errors. The solid lines represent squared Legendre polynomials with the L values shown, normalized to fit the data.

nuclei recoiling in the forward direction, or elastically scattered ^{16}O nuclei were analyzed in an Enge split-pole spectrograph. A resistive-wire ionization chamber[9] was used as focal-plane detector, providing position measurement and unambiguous particle identification. The backward-angle elastic and inelastic scattering angular distributions are shown in Fig. 4. In Fig. 5, the full angular distribution for the ^{16}O+^{24}Mg elastic scattering at $E_{c.m.}$ = 27.8 MeV is presented. Also shown in Fig. 5 are angular distributions of the ^{24}Mg(^{16}O,^{12}C)^{28}Si reaction to the ground- and first-excited states in ^{28}Si; these curves were obtained by combining the backward-angle data obtained

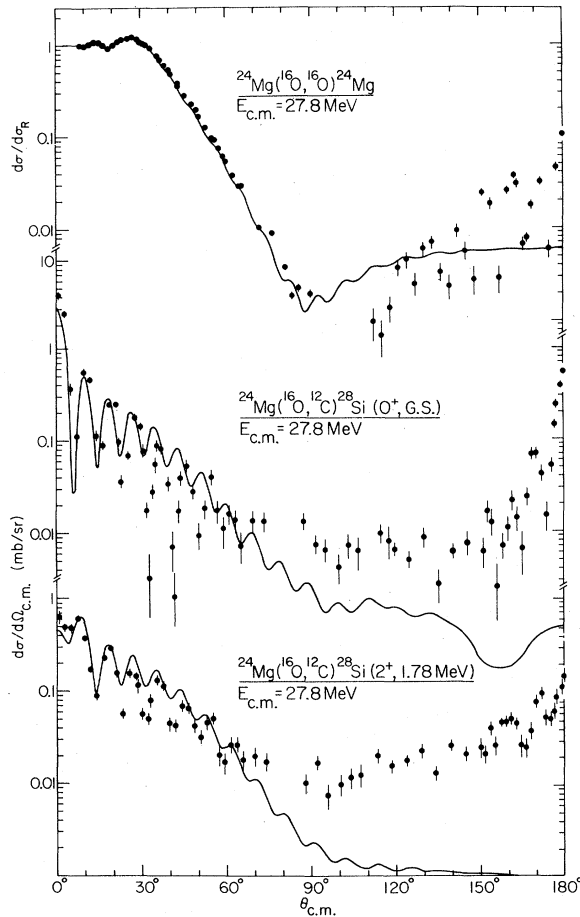FIG. 5. Full angular distributions of the ^{24}Mg(^{16}O,^{16}O) ^{24}Mg elastic scattering and the ^{24}Mg(^{16}O,^{12}C)^{28}Si(0$^+$,g.s.) and ^{24}Mg(^{16}O,^{12}C)^{28}Si(2$^+$,1.78 MeV) reactions. The elastic cross sections were measured using the ^{24}Mg(^{16}O,^{16}O)^{24}Mg reaction for 8°≤ $\theta_{c.m.}$ ≤ 90°, the ^{24}Mg(^{16}O,^{24}Mg)^{16}O reaction for 110°≤ $\theta_{c.m.}$ ≤ 170°, and the ^{16}O(^{24}Mg,^{16}O)^{24}Mg reaction for 160°≤ $\theta_{c.m.}$ ≤ 180°. Data at 0°≤ $\theta_{c.m.}$ ≤ 35° and at 35°≤ $\theta_{c.m.}$ ≤110° for the ^{24}Mg(^{16}O,^{12}C)^{28}Si(0$^+$, 2$^+$) reactions are taken from Refs. 3 and 9, respectively. The solid lines are results of optical-model and DWBA calculations (see text).

here with the data from Refs. 3 and 10.

Figure 5 shows the strong rise of the backward-angle yields of both the elastic and the transfer reactions. The ^{24}Mg(^{16}O, ^{16}O)^{24}Mg elastic cross section at $\theta_{c.m.}$ = 180° is about 10% of the Rutherford value. At back angles, angular distributions for transitions to the ground states of ^{28}Si and ^{24}Mg are strongly oscillatory. The angular distributions corresponding to the 2$^+$ states are somewhat smoother; some have a minimum at $\theta_{c.m.}$ = 180° (see Fig. 4).

III. DISCUSSION

The excitation functions shown in Fig. 2 for the ^{24}Mg(^{16}O, ^{12}C)^{28}Si and ^{24}Mg(^{16}O, ^{16}O)^{24}Mg reactions at 180° are similar in character to the recent results of Lee et al.[2] and Clover et al.[11] for $17 \leq E_{c.m.} \leq 31$ MeV; in the energy range of overlap, the positions of the maxima agree with our results. It has been noted previously[1] that excitation functions for the ^{12}C + ^{28}Si elastic and inelastic channels exhibit a pronounced fine structure on the scale of 250 keV. In the present results, for both the (^{16}O, ^{12}C) and (^{16}O, ^{16}O) reactions, the width of the observed structures is about 1 MeV in the center-of-mass system. However, the energy spread due to the target thickness, $\Delta E_{c.m.} \simeq 300$ keV, may have masked possible fine-structure effects.

The excitation functions for the elastic and inelastic channels (Fig. 2) show a very strong correlation in the position of their maxima. Such strong correlations have been observed previously in the elastic and inelastic scattering of ^{16}O on ^{28}Si[1] and more recently on ^{29,30}Si.[12] These correlations have been taken as an indication[1] of the existence of simple resonance mechanisms dominating the backward-angle scattering. In the present results, however, the structures in the ^{16}O+^{24}Mg elastic and inelastic scattering excitation functions are not obviously correlated with those seen for the (^{16}O, ^{12}C) channels, except perhaps for the peak observed near $E_{c.m.}$ = 27.8 MeV. In Table I, cross-correlation coefficients are given for the excitation functions of the ^{24}Mg(^{16}O, ^{12}C)^{28}Si reaction and of the ^{16}O+^{24}Mg and ^{12}C + ^{28}Si elastic and inelastic scattering. The data for the ^{12}C + ^{28}Si system were taken from Refs. 1 and 13. The coefficients were calculated using the expressions

$$S_{ij} = \frac{\langle d_i d_j \rangle}{\langle d_i^2 \rangle^{1/2} \langle d_j^2 \rangle^{1/2}},$$

$$d_i \equiv \frac{\sigma_i(E)}{\langle \sigma_i(E) \rangle_\Delta} - 1, \qquad (1)$$

where $\langle \sigma_i(E) \rangle_\Delta$ denotes the energy dependent average cross section[14] for the channel i, calculated

TABLE I. Cross-correlation coefficients (see text) for the 180° excitation functions of the ^{24}Mg(^{16}O, ^{12}C)^{28}Si reaction to the 0$^+$ ground state and 2$^+$ first-excited state in ^{28}Si and the ^{16}O+^{24}Mg and ^{12}C+^{28}Si elastic and inelastic scattering.

	^{24}Mg(^{16}O,^{16}O)^{24}Mg(2$^+$)	^{24}Mg(^{16}O,^{12}C)^{28}Si(0$^+$)	^{24}Mg(^{16}O,^{12}C)^{28}Si(2$^+$)	^{28}Si(^{12}C,^{12}C)^{28}Si(0$^+$)	^{28}Si(^{12}C,^{12}C)^{28}Si(2$^+$)
^{24}Mg(^{16}O,^{16}O)^{24}Mg(0$^+$)	0.61	0.12	-0.08	-0.39	0.15
^{24}Mg(^{16}O,^{16}O)^{24}Mg(2$^+$)		0.32	0.23	-0.11	0.05
^{24}Mg(^{16}O,^{12}C)^{28}Si(0$^+$)			0.38	0.06	0.21
^{24}Mg(^{16}O,^{12}C)^{28}Si(2$^+$)				0.18	-0.05
^{28}Si(^{12}C,^{12}C)^{28}Si(0$^+$)					-0.11

by averaging $\sigma(E)$ over an energy interval Δ; $\langle \ \rangle$ denotes the averaging over the whole energy range considered, $26.9 \leq E_{c.m} \leq 38.6$ MeV. Each excitation function consisted of 40 equally spaced data points (300 keV steps); where necessary, an interpolation procedure was employed to obtain the equal spacing. The averaging interval Δ was taken as 1.8 MeV; the results are not sensitive to this value. An additional smoothing was applied to attenuate the effect of the fine structure apparent in the excitation functions, especially prominent for the ^{12}C + ^{28}Si elastic and inelastic channels; the experimental cross sections were averaged over an interval of 0.9 MeV:

$$\sigma(E) = \frac{1}{0.9} \int_{E-0.45}^{E+0.45} \sigma_{exp}(E)dE$$

in Eq. (1). From an analysis of generated random spectra, it was determined that the 70% confidence level of a true correlation corresponds to a correlation coefficient of 0.25.

It appears from Table I that only the correlation coefficient between the elastic and inelastic ^{16}O+^{24}Mg channels is appreciable. The correlations between the (^{16}O, ^{12}C) reaction channels and either the ^{16}O+^{24}Mg or the ^{12}C+^{28}Si elastic channels are weak and, in contrast with the conclusion of Ref. 2, the present results do not seem to indicate that the ^{24}Mg(^{16}O, ^{12}C)^{28}Si resonant structures are governed by the entrance channel. In this context, it should be remembered that the existence of correlations between the structures seen in a reaction and the relevant elastic channels is not a necessary feature of a simple resonant process. Since the cross section of a pure resonant reaction is $\sigma \propto \Gamma_\alpha \Gamma_\beta$, where Γ_α and Γ_β are the partial widths of the resonant state in the entrance and exit channels, the dominant structures are determined by the overlap between the resonances in the two channels. For the two elastic channels, the cross sections for the same resonance are $\sigma_\alpha \propto \Gamma_\alpha^2$ and $\sigma_\beta \propto \Gamma_\beta^2$. The resonances seen strongly in the reaction must also contribute to the elastic cross sections, but they do not have to be the dominant structures.

Figure 6 shows a comparison between the experimental excitation functions of the (^{16}O, ^{12}C) reaction to the 0$^+$ and 2$^+$ states in ^{28}Si at forward angles[3] and the present data at backward angles. The forward-angle data of Ref. 3 have been corrected for the mean energy loss in the target, which was estimated to be ~800 keV in a reanalysis of these data. The backward-angle excitation curves were obtained by averaging the cross sections, as described previously, over an interval of 0.9 MeV to match approximately the energy averaging due to the target thickness in the for-
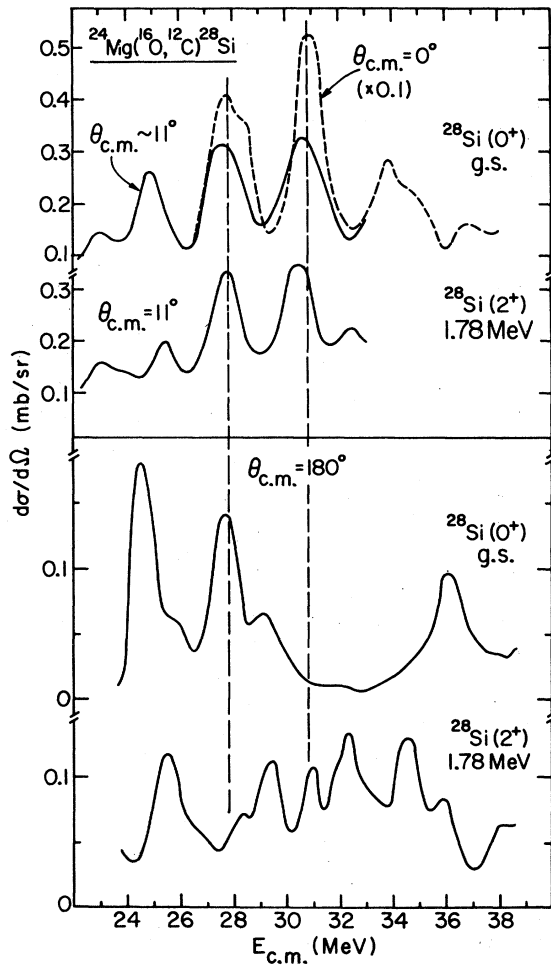
FIG. 6. Experimental excitation functions of the ^{24}Mg(^{16}O,^{12}C)^{28}Si reactions to the ground and first-excited states in ^{28}Si at forward angles (Ref. 3; upper part) and at $\theta_{c.m.} = 180°$ (present work; lower part). The 180° excitation curves were obtained by averaging the data of Fig. 2 over three adjacent energy steps, i.e., over a center-of-mass energy range of ~1 MeV to match the energy spread of the forward-angle data.

ward-angle measurement. It is noted in Fig. 6 that while the correlation between the 0$^+$ and 2$^+$ excitation functions is quite strong at forward angles, at backward-angles a correlation is not apparent. The strong peak in the forward-angle excitation functions at $E_{c.m.} \approx 28$ MeV also appears at backward angles for the (^{16}O,^{12}C) reaction and the ^{16}O+^{24}Mg elastic and inelastic scattering excitation functions (Figs. 2 and 6). At $E_{c.m.} \approx 31$ MeV, the forward-angle cross sections for the transfer reaction show a strong maximum which is not observed at 180°. This may be explained by an interference between close resonances, requiring the contribution of at least one even-J and one

odd-J resonance, interfering constructively at 0° and destructively at 180°. The assumption of interfering partial waves is confirmed by the behavior of the angular distribution of the (^{16}O,^{12}C) reaction at $E_{c.m.} = 30.8$ MeV, as shown below.

The presence of a resonance structure around $E_{c.m.} \approx 27.8$ MeV, as indicated both by the forward- and backward-angle data, is supported by the strong rise and the oscillatory behavior of the angular distributions of the various reactions at backward angles. In the forward-angle region, Erskine et al.[15] showed that the ^{24}Mg(^{16}O,^{12}C)^{28}Si angular distribution at $E_{c.m.} = 33.6$ MeV is fairly well described by distorted-wave Born-approximation (DWBA) calculations using the optical-model parameters ANL1 (see Table II). Although these parameters reproduce the shapes of the (^{16}O,^{12}C) angular distributions over a wide energy range, a fit to the present forward-angle elastic data at $E_{c.m.} = 27.8$ MeV (see Fig. 5) was made, using the ANL1 parameters as starting values and adjusting the real and imaginary potential geometry. The resulting parameters are listed in Table II as ANL1A. The DWBA calculations shown in Fig. 5 were performed with the code PTOLEMY[16] using the set ANL1A in both the entrance and exit channels. The calculated curves show some rise at backward angles, but neither the yield nor the oscillatory character of the data is reproduced. Some success was achieved recently[7] in reproducing the angular distributions and excitation functions in the backward-angle region for the ^{16}O+^{28}Si elastic scattering, using a surface-transparent potential with a parity-dependent absorption term. However, it is not yet clear how successful this approach is for other systems nor how it should be used in transfer calculations.

In Figs. 3 and 4, the angular distributions corresponding to the 0$^+$ state in ^{28}Si and ^{24}Mg are analyzed in terms of squared Legendre polynom-

TABLE II. Optical potential parameter sets for the system ^{16}O+^{24}Mg as discussed in the text. The optical potential $V(r)$ of Woods-Saxon shape is given in terms of the listed parameters by the following expressions:

$$V(r) = -V_0 f(r,R_r,a_r) - iW_0 f(r,R_i,a_i),$$
$$R_r = r_{0r}(A_1^{1/3}+A_2^{1/3}),$$
$$R_i = r_{0i}(A_1^{1/3}+A_2^{1/3}),$$
$$f(r,R,a) = \{1+\exp[(r-R)/a]\}^{-1}.$$

	V_0 (MeV)	r_{0r} (fm)	a_r (fm)	W_0 (MeV)	r_{0i} (fm)	a_i (fm)
ANL1	37	1.35	0.404	78	1.29	0.174
ANL1A	37	1.37	0.394	78	1.32	0.208

ials. At $E_{c.m.}$ = 27.8 MeV, both the elastic and the transfer angular distributions are reasonably well fitted by $P_{20}^2(\cos\theta)$ or $P_{21}^2(\cos\theta)$, but the quality of the fits suggests that more than a single partial wave contributes to the reactions. Also, it seems impossible from these fits alone to determine the main L value better than within $\pm 1\ \hbar$. This is illustrated in Fig. 7 where the χ^2 values of the fits of $P_L^2(\cos\theta)$ to the angular distributions are plotted as a function of the L value. While the partial waves contributing to these transitions are obviously close to each other, the fits do not determine whether, indeed, the same partial wave is dominant in the transfer reaction and in the elastic scattering. From their backward-angle measurement of the ^{24}Mg(^{16}O, ^{12}C)^{28}Si(g.s.) reaction at $E_{c.m.}$ = 28 MeV, Lee *et al.*[2] give a value of $L = 21$. Clover *et al.*[11] assign a value $L = 20$ to the $E_{c.m.}$ = 27.9 MeV angular distribution of the ^{16}O + ^{24}Mg elastic scattering at backward angles. Both these values are consistent with the present work; however, it should be noted that the excitation function of the ^{24}Mg(^{16}O, ^{12}C)^{28}Si(g.s.) reaction measured at $\theta_{c.m.}$ = 90° (Ref. 10) shows a maximum around $E_{c.m.}$ = 28 MeV and thus suggests that an even partial wave resonates at that energy, favoring a value of $L = 20$ or 22.

At $E_{c.m.}$ = 36.2 MeV, which corresponds to a strong maximum in the back-angle (^{16}O, ^{12}C) excitation function, the fit of $P_{26}^2(\cos\theta)$ to the 0$^+$-transfer angular distribution is excellent (Fig. 3) and the dependence of χ^2 upon the L value is much sharper as attested by Fig. 7. The data on the elastic ang-
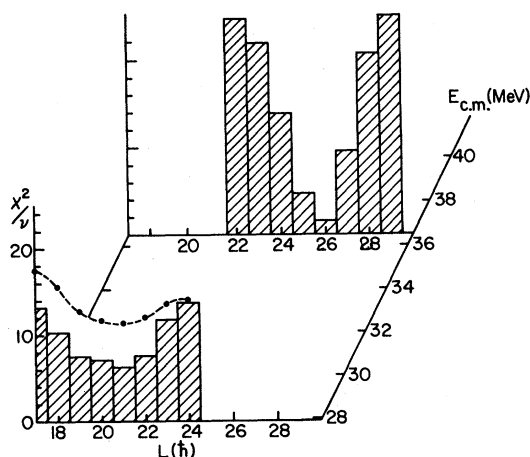

FIG. 7. Plot of the χ^2/(degree of freedom) of the fit of experimental angular distributions to $P_L^2(\cos\theta)$ as a function of L at $E_{c.m.}$ = 27.8 and 36.2 MeV. The histograms correspond to the ^{24}Mg(^{16}O, ^{12}C)^{28}Si(0$^+$, g.s.) reaction; the points correspond to the ^{16}O + ^{24}Mg elastic scattering.
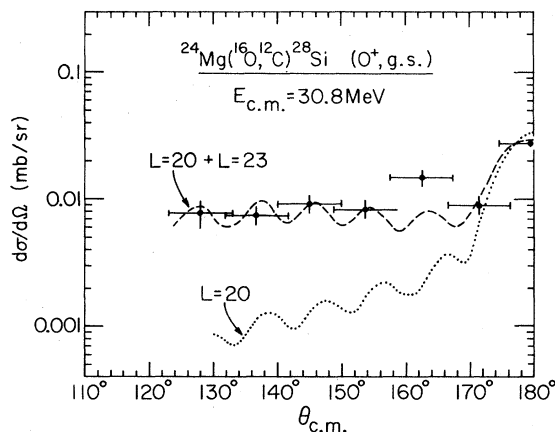
FIG. 8. Angular distributions of the ^{24}Mg(^{16}O, ^{12}C)^{28}Si-(0$^+$) reaction in the backward-angle region measured at $E_{c.m.}$ = 30.8 MeV. Horizontal bars represent the experimental angular aperture. The dashed line was obtained from the expression $|aP_{20}(\cos\theta) + bP_{23}(\cos\theta)|^2$, using $a = 0.445$ and $b = 0.216$, by averaging over the experimental angular aperture $\Delta\theta \simeq 10°$. The dotted line represents $P_{20}^2(\cos\theta)$ similarly averaged.

ular distribution at that energy, although limited, are consistent with an L value of 26.

At $E_{c.m.}$ = 30.8 MeV, the shape of the (^{16}O, ^{12}C) angular distribution (Figs. 3 and 8) differs from that of the previous cases. Although an oscillatory behavior may be masked by the averaging over the large angular aperture, the envelope to the true distribution is well defined by the data and differs drastically from the typical falloff of a P_L^2-like angular distribution, as exhibited at $E_{c.m.}$ = 27.8 and 36.2 MeV. This, together with the behavior of the excitation function discussed above, suggests the existence of a strong interference between different partial waves, as is qualitatively illustrated in Fig. 8. The dashed line shows an example of the angular distribution obtained by assuming the contribution of two partial waves with opposite parity, $L = 20$ and $L = 23$, as discussed for the excitation functions. The shapes obtained are rather insensitive to the actual values of the even and odd partial waves in the range $20 \le L \le 25$ and to small changes in the relative phase of their amplitudes. In Fig. 8, the shape of a pure $L = 20$ angular distribution is drawn for comparison of the falloff. Both lines were calculated by averaging over the range of angles ($\Delta\theta \simeq 10°$) corresponding to the experimental aperture.

IV. SUMMARY AND CONCLUSIONS

The 180° excitation functions of the ^{24}Mg (^{16}O, ^{12}C)^{28}Si and ^{24}Mg(^{16}O, ^{16}O)^{24}Mg reactions to the ground states and first-excited 2$^+$ states in

^{28}Si and ^{24}Mg reveal pronounced structures and a series of strong maxima, about 1 MeV wide, in the range $24 \lesssim E_{c.m.} \lesssim 40$ MeV. A cross-correlation analysis shows a high degree of correlation between the ^{16}O + ^{24}Mg elastic and inelastic scattering. The correlations between the (^{16}O, ^{12}C) reaction channels and either the ^{16}O + ^{24}Mg or ^{12}C + ^{28}Si elastic channels are weak. At $E_{c.m.} = 27.8$ MeV, a strong peak is seen in the ^{16}O + ^{24}Mg elastic, inelastic, and ^{24}Mg(^{16}O, ^{12}C)^{28}Si(g.s.) excitation functions at backward angles.

The angular distributions at $E_{c.m.} = 27.8$ and 36.2 MeV show a strong rise and an oscillatory shape at backward angles. At $E_{c.m.} = 27.8$ MeV, the main partial wave contributing to the backward-angle cross sections in the (^{16}O, ^{12}C) and (^{16}O, ^{16}O) reactions is $L = 20$ or 22. At $E_{c.m.} = 36.2$ MeV, $L = 26$ is predominant. At $E_{c.m.} = 30.8$ MeV, the excitation function and the angular distribution of the (^{16}O, ^{12}C) reaction suggest the existence of a strong interference between an even and odd partial wave.

In conclusion, the excitation functions and angular distributions of the ^{24}Mg(^{16}O, ^{12}C)^{28}Si reactions both at forward and backward angles show evidence for resonant structures. However, the backward-angle data presented in this work point to a complex situation where several resonances interfere. It is not possible, on the basis of the backward angle data only, to make unique assignments of J values.

*Present address: Dept. of Physics, Indiana Univ., Bloomington, Ind. 47401.

[1]J. Barrette, M. J. LeVine, P. Braun-Munzinger, G. M. Berkowitz, M. Gai, J. W. Harris, and C. M. Jachcinski, Phys. Rev. Lett. 40, 445 (1978).

[2]S. M. Lee, J. C. Adloff, P. Chevallier, D. Disdier, V. Rauch, and F. Scheibling, Phys. Rev. Lett. 42, 429 (1979).

[3]M. Paul, S. J. Sanders, J. Cseh, D. F. Geesaman, W. Henning, D. G. Kovar, C. Olmer, and J. P. Schiffer, Phys. Rev. Lett. 40, 1310 (1978).

[4]C. K. Gelbke, T. Awes, U. E. P. Berg, J. Barrette, M. J. LeVine, and P. Braun-Munzinger, Phys. Rev. Lett. 41, 1778 (1978).

[5]J. C. Peng, D. L. Hanson, J. D. Moses, O. W. B. Schult, Nelson Stein, J. W. Sunier, and N. Cindro, Phys. Rev. Lett. 42, 1458 (1979).

[6]J. Barrette, P. D. Bond, M. J. LeVine, and I. Tserruya, Bull. Am. Phys. Soc. 24, 570 (1979).

[7]D. Dehnhard, V. Shkolnik, and M. A. Franey, Phys. Rev. Lett. 40, 1549 (1978).

[8]See AIP document No. PAPS PRVCA-21-1802-22 for 22 pages of tabulations of the cross sections measured in the present work and in Ref. 10. Order by PAPS number and journal reference from American Institute of Physics, Physics Auxiliary Publication Service, 335 E. 45th Street, New York, N. Y. 10017. The price is $1.50 for microfiche, or $5 for photocopies. Airmail additional. Make checks payable to the American Institute of Physics. This material also appears in *Current Physics Microfilm*, the monthly microfilm edition of the complete set of journals published by AIP, on the frames immediately following this journal article.

[9]J. R. Erskine, T. H. Braid, and J. C. Stoltzfus, Nucl. Instrum. Methods 135, 67 (1976).

[10]S. J. Sanders, M. Paul, J. Cseh, D. F. Geesaman, W. Henning, D. G. Kovar, C. Olmer, and J. P. Schiffer, Phys. Rev. C 21, 1810(1980), following paper.

[11]M. R. Clover, B. R. Fulton, R. Ost, and R. M. DeVries, J. Phys. G 5, L63 (1979).

[12]P. Braun-Munzinger, G. M. Berkowitz, M. Gai, C. M. Jachcinski, T. Renner, C. D. Uhlhorn, J. Barrette, and M. J. LeVine, Bull. Am. Phys. Soc. 24, 571 (1979).

[13]P. Braun-Munzinger, G. M. Berkowitz, M. Gai, J. W. Harris, C. M. Jachcinski, C. D. Uhlhorn, J. Barrette, and M. J. LeVine (unpublished).

[14]G. Pappalardo, Phys. Lett. 13, 320 (1964).

[15]J. R. Erskine, W. Henning, D. G. Kovar, L. R. Greenwood, and R. M. DeVries, Phys. Rev. Lett. 34, 680 (1975).

[16]Code PTOLEMY, M. H. Macfarlane and S. C. Pieper, Argonne National Laboratory Informal Report No. ANL-76-11 Rev 1 (unpublished).